AGU PUBLICATIONS

JGR

Journal of Geophysical Research: Oceans

RESEARCH ARTICLE

10.1002/2013JC009710

Key Points:

- Altimetry-derived current products are evaluated using drifter observations
- Altimetry-based trajectory models perform better than numerical ocean models
- Altimetry products can provide essential information on ocean surface currents

Correspondence to:
Y. Liu,
yliu@mail.usf.edu

Citation:
Liu, Y., R. H. Weisberg, S. Vignudelli, and G. T. Mitchum (2014), Evaluation of altimetry-derived surface current products using Lagrangian drifter trajectories in the eastern Gulf of Mexico, *J. Geophys. Res. Oceans*, *119*, doi:10.1002/2013JC009710.

Received 9 DEC 2013
Accepted 18 APR 2014
Accepted article online 21 APR 2014

Evaluation of altimetry-derived surface current products using Lagrangian drifter trajectories in the eastern Gulf of Mexico

Yonggang Liu[1], Robert H. Weisberg[1], Stefano Vignudelli[2], and Gary T. Mitchum[1]

[1]College of Marine Science, University of South Florida, St. Petersburg, Florida, USA, [2]Consiglio Nazionale delle Ricerche, Area Ricerca CNR, Pisa, Italy

Abstract Lagrangian particle trajectory models based on several altimetry-derived surface current products are used to hindcast the drifter trajectories observed in the eastern Gulf of Mexico during May to August 2010 (the Deepwater Horizon oil spill incident). The performances of the trajectory models are gauged in terms of Lagrangian separation distances (*d*) and a nondimensional skill score (*s*), respectively. A series of numerical experiments show that these altimetry-based trajectory models have about the same performance, with a certain improvement by adding surface wind Ekman components, especially over the shelf region. However, their hindcast skills are slightly better than those of the data assimilative numerical model output. After 3 days' simulation the altimetry-based trajectory models have mean *d* values of 75–83 and 34–42 km (*s* values of 0.49–0.51 and 0.35–0.43) in the Gulf of Mexico deep water area and on the West Florida Continental Shelf, respectively. These satellite altimetry data products are useful for providing essential information on ocean surface currents of use in water property transports, offshore oil and gas operations, hazardous spill mitigation, search and rescue, etc.

1. Introduction

The Gulf of Mexico (GOM) became of national and international interest in spring-summer 2010 as a consequence of the Deepwater Horizon incident, the largest offshore oil spill in U.S. history. The complex, time varying ocean circulation of the region played an important role in advecting the oil from the spill site [e.g., *Liu et al*., 2011a]. On the northern side of the eastern GOM, the shelf currents are generally weaker and mostly wind-driven [e.g., *Mitchum and Sturges*, 1982; *Weisberg et al*., 2001, 2005; *Morey et al*., 2005]; however, on the southern side, deep ocean currents, embodied by the GOM Loop Current system (i.e., the Loop Current and its eddies), are much stronger [e.g., *Sturges and Lugo-Fernández*, 2005 and the chapters therein; *Chang and Oey*, 2013]. Thus, the Loop Current system (Figure 1) posed a threat to the potential expansion of the Deepwater Horizon disaster [e.g., *Weisberg*, 2011]. The Deepwater Horizon oil spill highlighted the need to build more complete, sustained and integrated coastal ocean observation systems, and to be prepared for rapid response to similar incidents in coastal oceans [*Liu et al*., 2011c, *Weisberg*, 2011]. Many observing tools—in water or in space—are required to collect data for both deep and coastal oceans.

In particular, radar altimeters from satellites are of beneficial use in ocean observing systems [e.g., *Fu and Chelton*, 1984; *Cipollini et al*., 2010; *Benveniste*, 2011]. They provide accurate estimates of the Sea Surface Height (SSH) for the world's ocean, through the analysis of echoes bounced back from the sea surface. Altimeter-derived Sea Level Anomaly (SLA) data are often used to infer surface geostrophic current anomalies, which are believed to be good approximations of surface current anomalies in deep ocean regions [e.g., *Lagerloef et al*., 1999; *Willis and Fu*, 2008]. There are several such altimetry-derived surface velocity products freely available for use, e.g., the Archiving, Validation and Interpretation of Satellite Oceanographic Data (AVISO) gridded product [e.g., *Pascual et al*., 2006], the Ocean Surface Currents Analyses Real-time (OSCAR) [e.g., *Bonjean and Lagerloef*, 2002; *Dohan and Maximenko*, 2010], and the Geostrophic and Ekman Current Observatory (GEKCO) [*Sudre et al*., 2013]. Some of these products are used to study large-scale circulation in the world's oceans [e.g., *Le Traon and Morrow*, 2001; *Lagerloef et al*., 2003; *Johnson et al*., 2007] and its semienclosed seas [e.g., *Cipollini et al*., 2008].

Since altimetry SSH maps provide essential information of large scale ocean thermodynamics, they are assimilated into numerical ocean circulation models to improve ocean current simulation [e.g., *Fox et al*., 2002]. There are several data assimilative numerical ocean circulation models in the GOM region, e.g., the

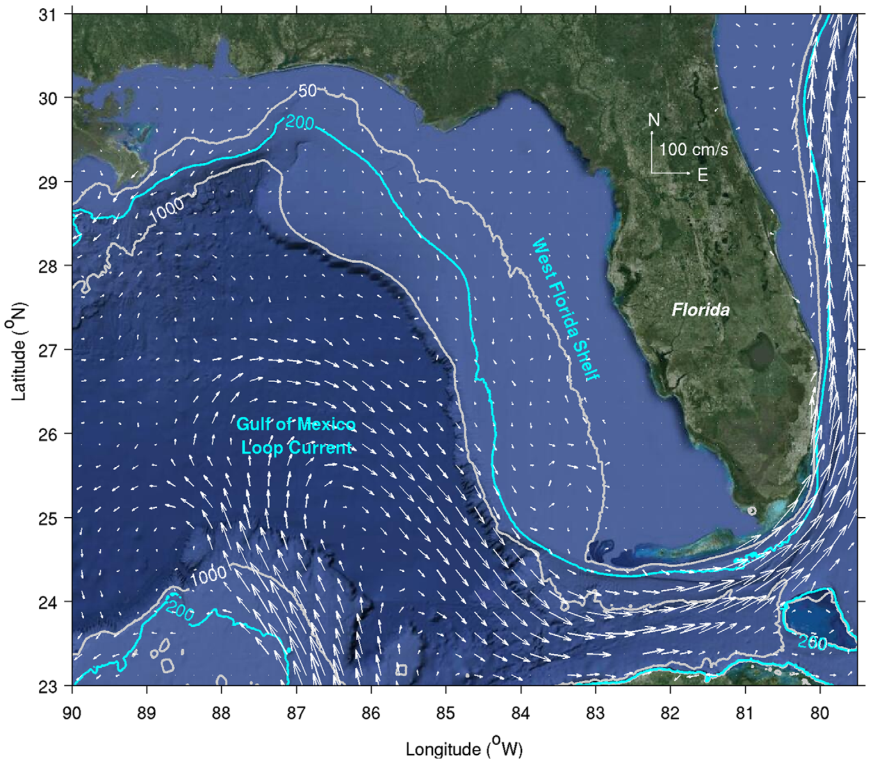

Figure 1. Map of the eastern Gulf of Mexico showing topography with isobaths of 50, 200, and 1000 m. Also superimposed are mean surface geostrophic currents derived from the mean dynamic topography of *Rio et al.* [2009].

Global Hybrid Coordinate Ocean Model (Global HYCOM) [*Chassignet et al.*, 2007]. Some of these model results are freely available for oceanographic applications. For example, the Global and GOM HYCOM outputs were employed in the surface oil trajectory modeling in response to the Deepwater Horizon incident [e.g., *Liu et al.*, 2011c]. It should be noted that the numerical ocean circulation model results have uncertainties due to a variety of reasons, such as accuracies of numerical schemes, parameterizations, and bathymetry, as well as initial conditions, surface and open boundary forcing fields.

Without being assimilated into models, altimetry products themselves, such as AVISO, OSCAR, and GEKCO, provide gridded surface current information with a temporal resolution of several days and spatial resolution of 1/3° or 1/4°. The altimetry data have also been used in describing the surface ocean circulation [e.g., *Jacobs and Leben*, 1990; *Leben and Born*, 1993; *Alvera-Azcárate et al.*, 2009], interpreting the movement of the surface oil slicks [e.g., *Liu et al.*, 2011b; *Hamilton et al.*, 2011; *Walker et al.*, 2011], and qualitatively validating the ocean circulation models [e.g., *Miller and Kuhn*, 2010] in the GOM. Since the altimetry products can be made available online near real-time, it would be useful to know the feasibility and usefulness of such operational applications.

The present analysis is a follow-on study of our trajectory modeling in response to the Deepwater Horizon oil spill based on the surface velocity fields output from data assimilative models [*Liu et al.*, 2011c]. It is also continuation of our altimetry data evaluation using in situ ADCP and HF radar measurements in the eastern GOM [*Liu et al.*, 2012]. Here we present results from running a Lagrangian particle trajectory model based on the altimetry-derived surface currents to hindcast the surface drifter trajectories in the eastern GOM observed during summer 2010. The purpose is to examine the usefulness of the altimetry data products themselves, relative to the numerical model outputs, in providing surface meso and large-scale ocean circulation that are essential in offshore oil exploration and operations, oil spill mitigation, and coastal pollution/property transport. The rest of the paper is arranged as follows: Data sets are described in section 2; trajectory model and its evaluation methods are provided in section 3; results are reported in section 4, with a summary in section 5.

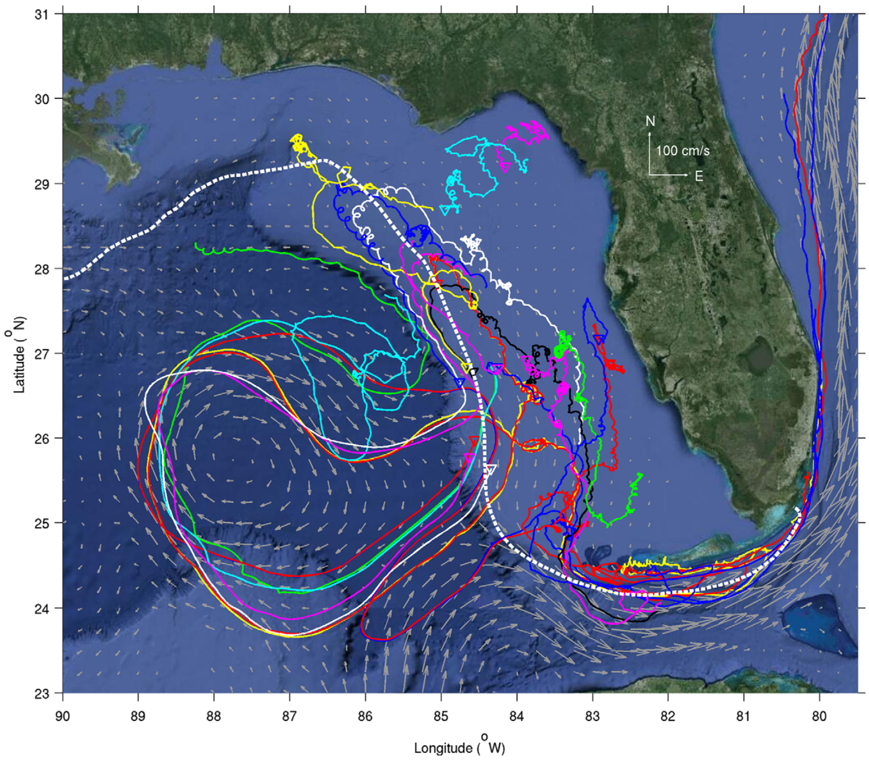

Figure 2. Satellite-tracked drifter trajectories collected by University of South Florida during May to August 2010 in the eastern Gulf of Mexico. Drifter trajectories are differentiated with various colors. Triangles designate the drifter release locations. Superimposed are the mean surface geostrophic currents derived from the AVISO gridded altimetry product during the same time period. The white dashed line indicates the open boundary of the West Florida Coastal Ocean model (WFCOM). This figure is modified from *Liu and Weisberg* [2011].

2. Data

2.1. Drifter Data

Satellite-tracked surface drifters are widely used in Lagrangian ocean observations [e.g., *Davis*, 1985; *Winant et al.*, 1999; *Fratantoni*, 2001; *McClean et al.*, 2002]. Extensive drifter applications were previously made in the GOM [e.g., *Yang et al.*, 1999; *Lugo-Fernandez et al.*, 2001; *Fan et al.*, 2004; *DiMarco et al.*, 2005; *Price et al.*, 2006], with many of these focusing on the Loop Current and its eddies [e.g., *Kirwan et al.*, 1988; *Hamilton et al.*, 1999; *Kuznetsov et al.*, 2002; *LaCasce and Ohlmann*, 2003]. Drifter trajectory data are also used for validating mesoscale circulation mapping by satellite altimetry [e.g., *Le Traon and Hernandez*, 1992] and interpreting Lagrangian Coherent Structures derived from altimetry data [*Olascoaga et al.*, 2013].

As a part of its response to the Deepwater Horizon oil spill efforts, University of South Florida (USF) deployed 18 satellite-tracked drifters in the GOM Loop Current region and on the West Florida Shelf (WFS) during May to August 2010, assisted by scientists from Florida Department of Environmental Protection (FDEP), U.S. Coast Guard (USCG), Florida Wildlife Research Institute (FWRI), Florida Institute of Technology (FIT), Woods Hole Oceanographic Institution (WHOI), and Northeast Fisheries Science Center (NEFSC). The surface drifters (drogued at 1 m depth) transmitted data via satellite in real time. The drifter trajectories are shown in Figure 2. Some of the drifters stayed on the WFS for a long time, others got entrained into the GOM Loop Current and its eddies and were transported eastward through the Florida Straits to the Atlantic coast. The locations of the drifters were binned into hourly time series and archived. Detailed information about the drifter data can be seen in *Liu et al.* [2011b]. This drifter data set was also used to assess the performance of a trajectory model that was employed to track the spilled oil [*Liu and Weisberg*, 2011], to describe the ocean circulation along with altimetry-derived surface geostrophic currents and ocean color imagery [*Liu et al.*, 2011b; *Hamilton et al.*, 2011], and to examine Lagrangian predictability from HF radar observations and model output [*Yaremchuk et al.*, 2014].

2.2. Altimetry Data

Several research groups reprocess altimetry data and produce altimetry-derived surface current velocity data in regional and global domains. Among these groups, the AVISO, OSCAR, and GEKCO offer gridded surface current data on global coverage, which allow us to extract data for the GOM region.

One of the AVISO altimetry products is the Ssalto/*Duacs* Gridded SLA and geostrophic velocity anomalies on a global grid of 1/3° resolution. The weekly data are produced by Ssalto/*Duacs* by merging multisatellite altimeter missions [e.g., *Ducet et al*., 2000; *Le Traon et al*., 2003]. All standard corrections were made by AVISO to account for wet troposphere, dry troposphere, and ionosphere delays, inverted-barometer and dynamic atmosphere responses, sea state bias, and ocean, solid earth and pole tides. The data are distributed by AVISO (http://www.aviso.oceanobs.com/duacs/), with support from the Centre National d'Etudes Spatiales (CNES). Both delayed-time and near real-time versions of the gridded SLA are available. It is generally expected that the delayed-time data are more precise than the near real-time counterparts. The AVISO products have been widely used to study ocean circulation variability at different scales [e.g., *Han*, 2007; *Liu et al*., 2008].

The AVISO gridded SLA product needs to combine with a mean dynamic topography (MDT), mean sea surface above geoid, to get absolute SSH. *Rio et al*. [2009] provided a combined MDT, called CNES-CLS09 MDT, based on 4.5 years of GRACE data, 15 years of altimetry, in situ hydrologic, and drifter data [*Rio et al*., 2011]. This is an updated version of MDT series [e.g., *Rio and Hernandez*, 2004; *Rio et al*., 2007]. This MDT is added to the AVISO gridded SLA to obtain absolute SSH for the eastern GOM region, from which we compute absolute geostrophic current velocity at sea surface. The mean surface geostrophic currents derived from the *Rio et al*. [2009] data are shown in Figure 1, which is an updated version of that in *Weisberg et al*. [2009].

Another MDT data set for the GOM region comes from the Miami Isopycnic Coordinate Ocean Model (MICOM) [e.g., *Bleck et al*., 1992; *Chassignet and Garraffo*, 2001], which is used by the USF Ocean Circulation Group in a near real-time regional SSH product. An automated surface geostrophic current and virtual drifter trajectory analysis is available online (http://ocgweb.marine.usf.edu/Products/Drifters), beginning with applications to advection of surface borne materials from Hurricane Katrina damage in September 2005. This product was used to examine the surface ocean circulation in the Caribbean Seas and GOM region [*Alvera-Azcárate et al*., 2009], to determine connectivity time scales between regions [e.g., *Weisberg*, 2011], and to study the GOM Loop Current and its eddies during the Deepwater Horizon oil spill incident [*Liu et al*., 2011b]. This MICOM mean field is added to the AVISO delayed-time SLA to get the absolute SSH, and then the surface absolute geostrophic current velocity.

The OSCAR product, developed at Earth and Space Research (ESR), provides near real-time ocean surface velocities from satellite fields on global grid of 1/3° resolution with a 5 day interval [e.g., *Lagerloef et al*., 1999; *Johnson et al*., 2007; *Dohan et al*., 2010]. This product is a direct computation of global surface currents using satellite SSH, scatterometer winds, and both Advanced Very High Resolution Radiometer (AVHRR) and in situ sea surface temperatures [*Bonjean and Lagerloef*, 2002]. Currents are calculated using a quasi-steady geostrophic model together with an eddy viscosity based wind-driven ageostrophic component and a thermal wind adjustment. So the OSCAR sea surface currents are actually averaged over the top 30 m of the upper ocean. The OSCAR data are also freely available through two data centers operated by NOAA and NASA JPL Physical Oceanography DAAC, respectively. *Johnson et al*. [2007] compared the OSCAR sea surface currents with in situ data from moored current meters, shipboard current profilers, drifters, and velocity output from a data-assimilating ECCO model (Estimating the Circulation and Climate of the Ocean) for the near-equatorial region. The comparison with drifter data is in terms of Eulerian velocity components. Recently, *Robinson* [2011] also evaluated the OSCAR product with in situ data from tide gauges, moored and shipboard ADCP measurements in the Intra-American Seas, including the eastern GOM. The OSCAR product has also been used to study ocean circulation variability at different scales [e.g., *Picaut et al*., 2002; *Legeckis et al*., 2004; *Lumpkin et al*., 2010], including an application in the Tropical Atlantic [*Helber et al*., 2007].

The GEKCO product, developed in the Centre de Topographie des Océans et de l'Hydrosphère (CTOH) at LEGOS, France, is another altimetry-derived surface current velocity data set [*Sudre and Morrow*, 2008; *Sudre et al*., 2013]. The velocity data are on global grid of 1/3° resolution with daily time stamp. Similar to the OSCAR data, the GEKCO total surface velocity data include surface geostrophic and wind Ekman components. The Ekman currents are derived from wind estimates from QuickSCAT satellite, and the geostrophic currents from the AVISO altimetry, with mean geostrophic currents derived from *Rio et al*. [2007]. Recently, the GEKCO estimates were compared with independent observations from both Lagrangian and Eulerian perspectives [*Sudre et al*., 2013].

Auxiliary data include winds reanalysis product from the NOAA National Centers for Environmental Prediction —North American Mesoscale model (NCEP NAM) [*Rogers et al*., 2009]. The surface Ekman velocity components will be added to the surface geostrophic velocity of the AVISO products to determine total surface currents, with the assumption that the near-surface velocity field can be decomposed into a geostrophic component and a wind-driven part. The surface Ekman current components (u_e, v_e) are calculated as

$$u_e = \frac{0.0127}{\sqrt{\sin(\phi)}} U_{10} \cos(\theta - \pi/4)$$
$$v_e = \frac{0.0127}{\sqrt{\sin(\phi)}} U_{10} \sin(\theta - \pi/4), \quad (1)$$

where U_{10} and θ are the 10 m wind speed and direction, respectively, and φ is the latitude [*Stewart*, 2008].

2.3. Model Output

Several numerical ocean circulation model outputs were used in the nowcast/forecast of the oil spill trajectories in a rapid response to the Deepwater Horizon oil spill incident [*Liu et al*., 2011c]. Among these models, the Global HYCOM, the GOM HYCOM, and the Intra America Seas Nowcast/Forecast System (IASNFS) [*Ko et al*., 2003] are data assimilative, and the model outputs are still freely available online.

The Global HYCOM, combined with the Navy Coupled Ocean Data Assimilation (NCODA) system [*Cummings*, 2005], provides daily snapshots of ocean currents hindcast on a 1/12° horizontal grid. The NCODA assimilates available along-track satellite altimetry data, satellite and in situ sea surface temperature data as well as available in situ vertical temperature and salinity profiles from XBTs, ARGO floats and moored buoys. Surface forcing, including wind stress, wind speed, heat flux, and precipitation comes from Navy Operational Global Atmospheric Prediction System (NOGAPS) [*Rosmond et al*., 2002]. The Global HYCOM + NCODA analysis system is a popular source of open boundary forcing for limited-domain coastal ocean circulation models [e.g., *Barth et al*., 2008]. The GOM HYCOM is similar to the Global HYCOM but focuses on the GOM region with higher horizontal resolution (1/25°). Both the Global and GOM HYCOM outputs are freely available at the HYCOM Consortium website (www.hycom.org).

The IASNFS is an experimental real-time ocean nowcast/forecast system developed based on the Navy Coastal Ocean Model (NCOM) and one-way nested within the Global NCOM [*Ko et al*., 2003, 2008; *Barron et al*., 2006]. It has a horizontal grid of 1/24° degree (~6 km), combines with the NCODA data assimilative system, and uses surface forcing from the NOGAPS. It is operated at the Naval Research Laboratory with daily model output served through the Northern Gulf Institute (northerngulfinstitute.org).

Recently, the USF Ocean Circulation Group implemented a West Florida Coastal Ocean model (WFCOM) by nesting the unstructured grid, Finite Volume Coastal Ocean Model (FVCOM) [*Chen et al*., 2003] in the HYCOM to downscale from the deep ocean, across the continental shelf and into the estuaries without the need for multiple nesting [*Zheng and Weisberg*, 2012]. The WFCOM presently uses the GOM HYCOM for its open boundary forcing. The horizontal grid size varies from ~6 km near the open boundary to ~150 m in the estuaries. Surface forcing comes from the NOAA NCEP NAM reanalyzed winds and surface heat. It also includes eight tidal constituents as forcing along the open boundary. Hourly model hindcast outputs are archived for further analysis [e.g., *Weisberg et al*., 2014].

3. Lagrangian Trajectory Model and Evaluation

Lagrangian particle-tracking is often found in oceanographic applications [e.g., *Edwards et al*., 2006; *Barron et al*., 2007; *Sotillo et al*., 2008; *Abascal et al*., 2009; *Wei et al*., 2014]. A Lagrangian trajectory model, based on the surface velocity fields output from six numerical circulation models, played an important role in the rapid response to the Deepwater Horizon oil spill [e.g., *Liu et al*., 2011c, 2011d]. The model uses a trilinear interpolation scheme in longitude, latitude, and time to interpolate the surface velocity time series. It simulates particle positions using a fourth-order Runge-Kutta algorithm for time integration [e.g., *Hofmann et al*., 1991]. Two measures will be used to quantitatively evaluate the trajectory hindcast: (1) the Lagrangian separation distance (d), defined as the separation distance between the end points of the simulated and observed Lagrangian trajectories and (2) the skill score (s):

$$s=\begin{cases} 1-\dfrac{c}{n}, & (c \le n) \\ 0, & (c > n) \end{cases}, \tag{2}$$

as proposed in *Liu and Weisberg* [2011], where n is a tolerance threshold, c is a normalized cumulative Lagrangian separation distance, i.e., the cumulative Lagrangian separation distance (d) divided by the cumulative length of the observed trajectory (l)

$$c=\sum_{i=1}^{N} d_i \Big/ \sum_{i=1}^{N} l_i, \tag{3}$$

where $i = 1, 2, \ldots, N$, and N is the total number of days. As discussed in *Liu and Weisberg* [2011], the tolerance threshold n defines the expectations/requirements to the model. A larger n value corresponds to a lower expectation, while a smaller n value indicates a stricter requirement. In assessing performance of a model, it is important to reassess the model's aim and scope, and properly select performance criteria [*Bennett et al*., 2013]. We follow the suggestion of *Liu and Weisberg* [2011], and select the tolerance threshold $n = 1$. Thus, the skill score is simplified as

$$s=\begin{cases} 1-c, & (c \le 1) \\ 0, & (c > 1) \end{cases}. \tag{4}$$

In this case, model simulations with $c > 1$ are flagged to be no skill ($s = 0$), which corresponds to a criterion that, to be acceptable, the cumulative separation distance should not be larger than the cumulative length of the trajectory. The highest score ($s = 1$) indicates perfect skill.

This nondimensional skill score correctly indicates the relative performance of the Global HYCOM in modeling the strong currents of the GOM Loop Current and the Gulf Stream and the weaker currents on the WFS. In contrast, the Lagrangian separation distance (d) alone gives a misleading result [*Liu and Weisberg*, 2011]. This skill score is particularly useful when the number of drifter trajectories is limited and neither a conventional Eulerian-based velocity nor a Lagrangian based probability density function may be estimated [e.g., *Garaffo et al*., 2001; *Toner et al*., 2001; *Griffa et al*., 2007; *Ohlmann and Mitarai*, 2010]. The skill assessment is solely based on the drifter trajectories, and thus prior knowledge of the ocean circulation in the interested region or additional climatological data of the mean circulation patterns are not required [e.g., *Özgökman et al*., 2000]. These features make the skill score a practical index for model evaluation. Recently, it finds applications in assessing numerical ocean circulation models [e.g., *Mooers et al*., 2012; *Halliwell et al*., 2014]. It also gains popularity in evaluating trajectory models for oil spill and search and rescue operations [*Röhrs et al*., 2012; *Ivichev et al*., 2012; *De Dominicis et al*., 2013; *Sayol et al*., 2014; *Janeiro et al*., 2014]. Recently, it has been extended to use a cluster of particles to get a mean skill score in the evaluation of an altimetry-derived currents [*Bouffard et al*., 2014]. This skill score is a good addition to the model performance methods summarized by *Bennett et al*. [2013].

For each drifter trajectory, a virtual particle is released/reinitialized daily at the observed location, and tracked in the model based on the altimetry-derived current velocities. For each reinitialization, both the Lagrangian separation distance (d_3) and the skill score (s_3) are calculated after 3 days simulation, following *Liu and Weisberg* [2011]. This results in daily series of d_3 and s_3 along a drifter trajectory. Figure 3 shows an example of simulated particle trajectories and the corresponding model skill scores s_3. Generally, higher skill scores ($s_3 \sim 0.8$) correspond to better agreement between the simulated and the observed trajectories, which is seen during 12–18 June 2010 (Figure 3). The lower skill scores ($s_3 < 0.1$) are found for 23–24 June 2010 near the shelf break where the simulated particle tends to drift away from the observed drifter

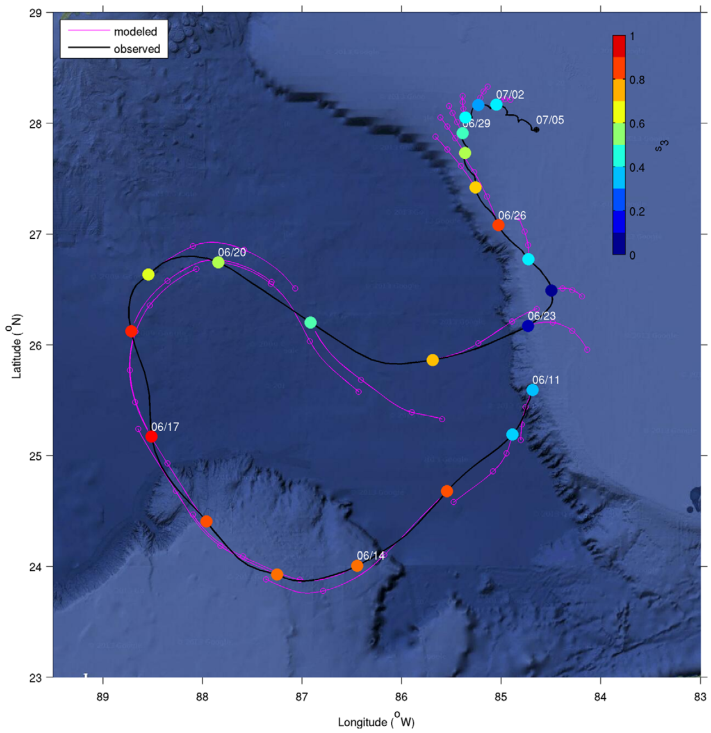

Figure 3. Observed (black) and simulated (magenta) trajectories along a drifter path in the eastern Gulf of Mexico. The trajectory model reinitializes daily from the observed drifter locations. Open circles represent daily simulated drifter locations and closed circles (color-coded) designate the model skill scores after 3 days' simulation (s_3).

trajectory, even in the opposite direction (Figure 3). So the skill score s_3 properly indicates the trajectory model performance during the 3 day period.

4. Results

We perform a series of Lagrangian trajectory model simulations based on the surface currents derived from the altimetry products and output from the data assimilative numerical ocean circulation models. The numerical experiments are listed in Table 1. The altimetry-based trajectory models include the two versions (near real-time and delayed time) of AVISO gridded data in combination with a mean SSH or MDT (the MICOM model mean SSH or the Rio 2009 MDT), the OSCAR, and the GEKCO products. Note that both the OSCAR and the GEKCO current products include wind Ekman components, while the AVISO products do not. Surface Ekman currents are added to the surface geostrophic currents to examine whether there are improvements in the surface trajectory simulation in the Loop Current region. The data-assimilative model-based trajectory simulations include the Global and GOM HYCOM, and the NCOM IASNFS. The WFCOM is also used to simulate the trajectories on the WFS.

4.1. Altimetry Products

Figure 4 shows the spatial distribution of the skill scores (s_3) of the altimetry based trajectory models. For the AVISO + MICOM mean SSH product (Figure 4a), the skill scores are generally higher ($s_3 > 0.4$) in the deep water area in the center of the GOM, with the highest skill scores ($s_3 = 0.8$–0.9) located in the western part of the GOM Loop Current anticyclonic eddy. Although sporadic high skill scores are also seen on the

Table 1. Trajectory Model Performances After 3 Days Simulation

	Mean Separation Distance (d_3) (km)		Mean Skill Score (s_3)	
Trajectory Model Type	Ocean	Shelf	Ocean	Shelf
(1) AVISO (near real-time) + MICOM mean	83	42	0.49	0.36
(2) AVISO (delayed time) + MICOM mean	83	42	0.49	0.37
(3) AVISO (delayed time) + MICOM mean + Ekman	75	34	0.50	0.43
(4) AVISO (delayed time) + Rio2009 mean	78	41	0.50	0.35
(5) AVISO (delayed time) + Rio2009 mean + Ekman	76	36	0.50	0.41
(6) OSCAR	79	39	0.49	0.37
(7) OSCAR (maximum mask)	78	40	0.50	0.36
(8) GEKCO	76	37	0.51	0.38
(9) Global HYCOM	88	39	0.41	0.36
(10) Gulf of Mexico HYCOM	91	41	0.38	0.33
(11) IASNFS	105	38	0.34	0.36
(12) WFCOM		38		0.39

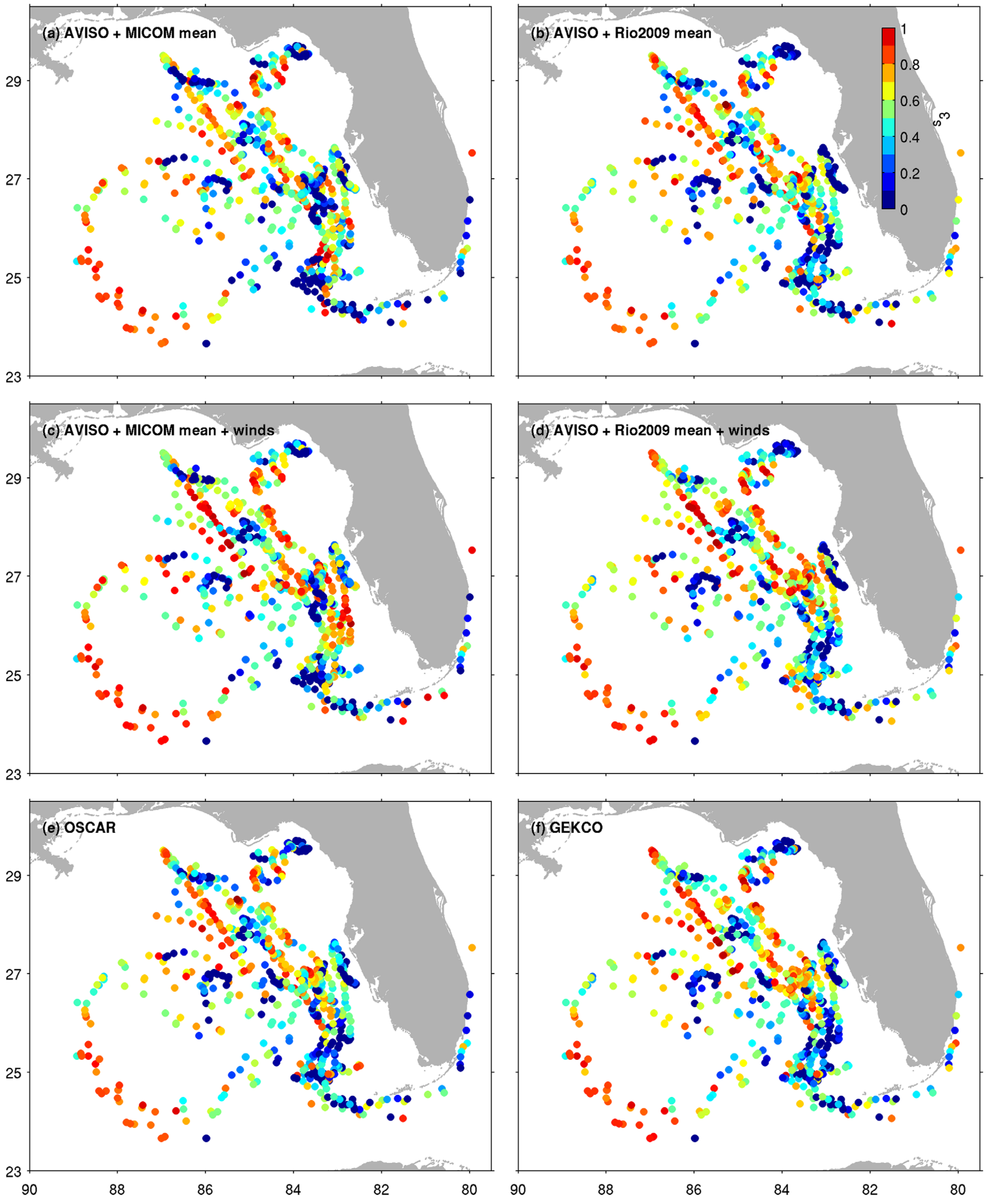

Figure 4. Spatial distribution of the trajectory model skill scores (s_3) in the eastern Gulf of Mexico based on different altimetry-derived surface current products: surface geostrophic velocity derived from (a) the AVISO (delayed-time) SLA plus MICOM model mean dynamic topography, (b) the AVISO (delayed-time) SLA plus mean dynamic topography produced by *Rio et al*. [2009], (c) same as (a) but with surface wind Ekman currents, (d) same as (b) but with surface wind Ekman currents, (e) the OSCAR product, and (e) the GEKCO product.

WFS, the skill scores in the shallow water area toward the WFS are generally lower than those in the deep water area. Since the skill score difference between the near real-time and the delayed time AVISO products is visually unnoticeable, only the results of the delayed time AVISO product are shown in Figure 4a. The

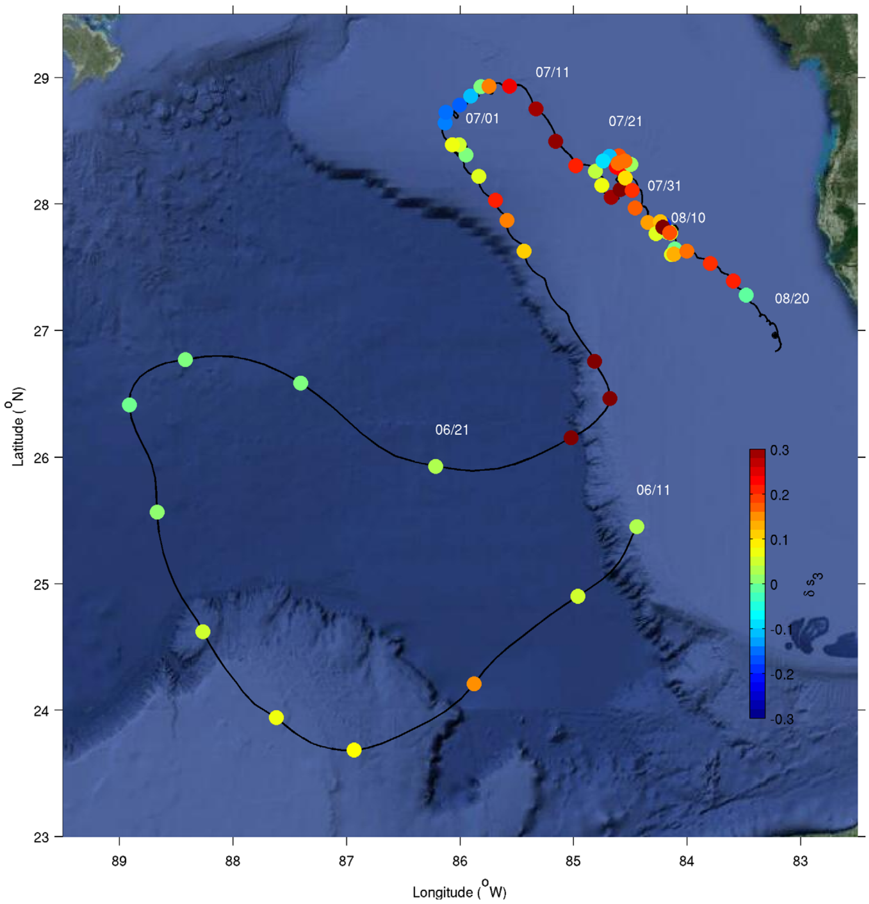

Figure 5. The skill score differences (Δs_3) between the altimetry (AVISO + Rio2009) derived surface geostrophic currents with and without the surface Ekman currents. Positive values of Δs_3 indicate improvement of the trajectory simulation after winds are included. The trajectory is labeled every 10 days since 11 June 2010.

AVISO + Rio 2009 MDT product has a similar skill score pattern as the AVISO + MICOM mean SSH product, and the difference between the two products is minor and mainly located in the eastern part of the trajectories (Figure 4b). Adding surface Ekman components to the AVISO products generally increase the skill scores for the WFS area where the water depths are generally shallow (Figures 4c and 4d). An example of such improvement in trajectory modeling is shown in Figure 5. Along this drifter trajectory, we see more positive changes of the skill scores on the shelf than in the deep ocean area. Both the OSCAR and the GEKCO products have similar skill score patterns as the AVISO products, i.e., generally higher skill scores in the deep water area and lower skill scores on the WFS (Figures 4e and 4f).

4.2. Data Assimilative Models

Figure 6 shows the spatial distribution of the skill scores (s_3) of the trajectory simulation based on the surface currents output from the three data assimilative ocean circulation models (the two HYCOMs and the IASNFS). Similar to those of the altimetry-based trajectory models, the skill scores are generally higher in the GOM Loop Current eddy region and lower on the WFS to the east. A major difference is the lower skill scores ($s_3 < 0.2$) appearing in the transition area from the deep ocean to the shelf (Figures 6a,–6c). Their counterparts in the altimetry-derived products are generally high ($s_3 > 0.7$). A closer examination of the simulated trajectories based on the currents derived from the altimetry product and output from the numerical ocean circulation model confirmed the differences in model skills (Figure 7). During the 12 days' period (8–20 June 2010), the AVISO-based trajectories generally tend to follow the direction of the observed drifter path in the along-slope direction, while the Global HYCOM-based trajectories tend to

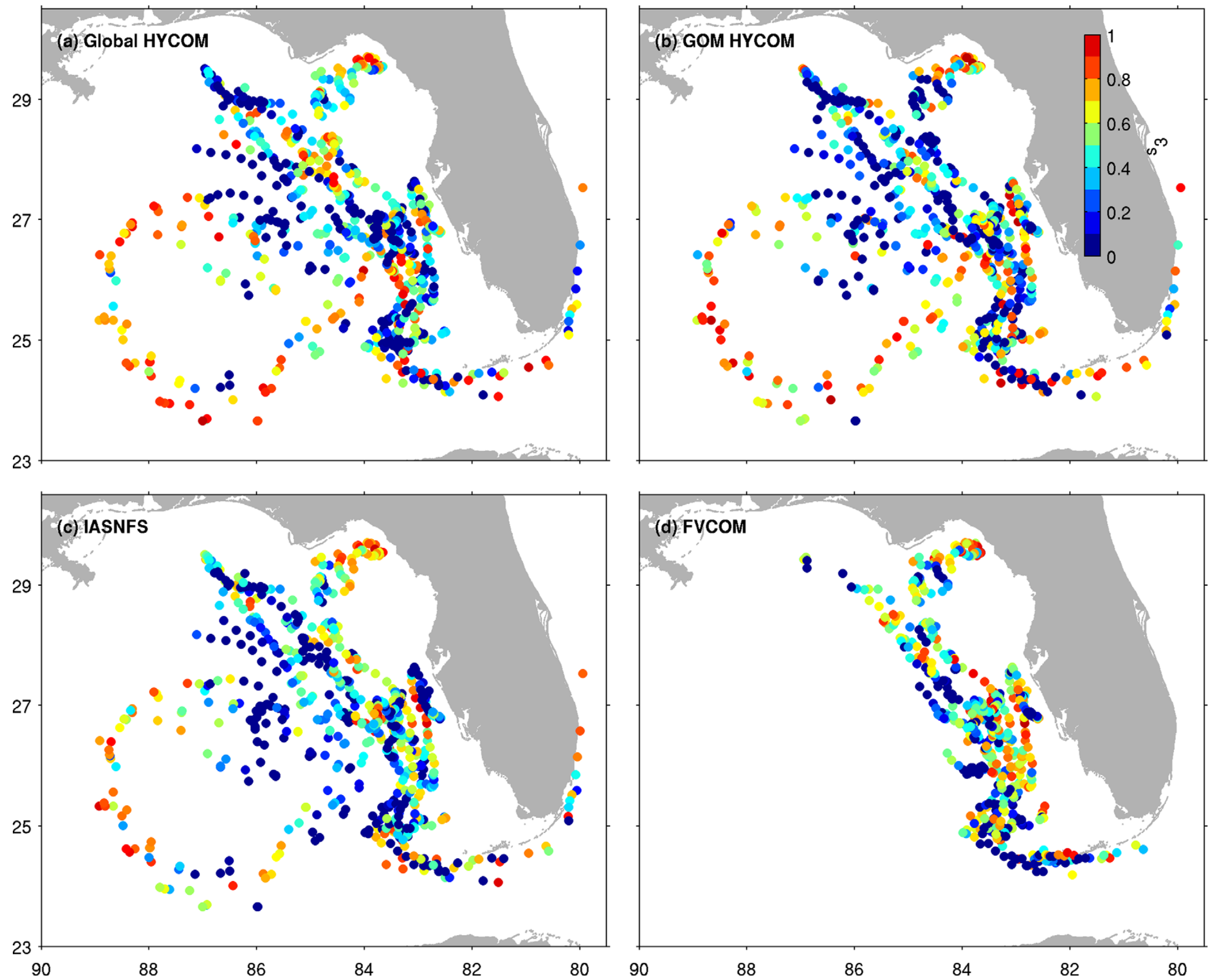

Figure 6. Spatial distribution of the trajectory model skill scores (s_3) in the eastern Gulf of Mexico based on the surface currents output from different ocean circulation models: (a) the Global HYCOM, (b) the Gulf of Mexico HYCOM, (c) the IASNFS, and (d) the WFCOM. Note that only the drifters located within the WFCOM domain are shown in (d).

deviate from the observed drifter moving direction. This finding suggests that the data assimilative models may need some improvement for this transition region. It may be due to inadequate coverage of data being assimilated into the models. It should be noted that conventional altimetry data are not reliable near the coasts [e.g., *Vignudelli et al*., 2011; *Birol and Delebecque*, 2014], and the cutoff of the altimetry data in coastal region may be too large.

4.3. Deep Ocean Versus Shelf

The dominant ocean circulation dynamics are different in the open ocean area and on the shelf. In the GOM Loop Current region, the currents are much stronger (by an order of magnitude) than those on the shelf and the geostrophic component may be dominant in the surface currents [e.g., *Oey et al*., 2005; *Liu et al*., 2011b]. In contrast, the weaker currents on the shelf may at times be mostly driven by local winds [e.g., *Weisberg et al*., 2005; *Liu and Weisberg*, 2005, 2007]. It is necessary to examine the model performance separately for the two dynamically distinct regions. The observed drifter trajectories are roughly classified into two categories (deep ocean and shelf) in terms of the open boundary line of the WFCOM. The drifter trajectories within the WFCOM domain are regarded as on the shelf, while those outside of the shelf model domain are treated as in the ocean. Both mean Lagrangian separation distance (d_3) and mean skill score (s_3) after 3 days simulation are calculated for each numerical experiment (Table 1). These mean values quantify the relative performance of the trajectory models.

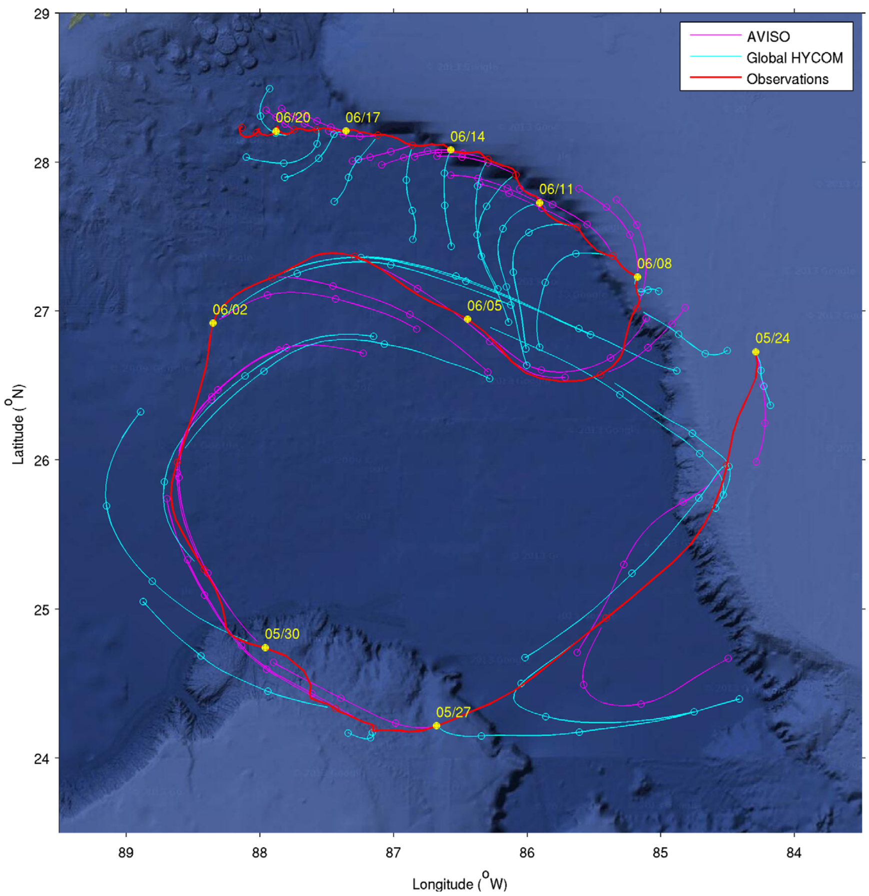

Figure 7. Comparison of observed (red) and simulated surface drifter trajectories based on the surface currents derived from the AVISO product (magenta) and output from the Global HYCOM (cyan), respectively. The open circles designate daily simulated drifter locations. The observed drifter trajectory is labeled every 3 days from 24 May to 20 June 2010.

All the altimetry-based trajectory models have about the same performance, with mean d_3 values of 75–83 km (34–42 km) and mean s_3 values of 0.49–0.51 (0.36–0.43) in the deep ocean area (on the shelf). Those based on the numerical ocean circulation models have mean d_3 values of 88–105 km (38–41 km) and mean s_3 values of 0.34–0.41 (0.33–0.36) in the deep ocean area (on the shelf). Note that smaller d_3 and larger s_3 indicate better model performance. According to d_3, these models have better performance on the shelf than over the deep ocean, while in terms of s_3, these models have better skills over the deep ocean than on the shelf. The skill score is a more acceptable metric in assessing the model in a region of distinct ocean dynamics [*Liu and Weisberg*, 2011]. Note that conventional altimetry products may not be reliable near the coast [e.g., *Vignudelli et al*., 2011], also their temporal sampling (weekly maps) is not high enough to resolve synoptic variation of the coastal circulation [e.g., *He et al.*, 2004]. Thus, the comparison will be mainly focused on the deep ocean region. It is interesting that the altimetry-based trajectory models perform slightly better, i.e., they have smaller d_3 and larger s_3 values, than those based on the data assimilative ocean circulation models.

We use the daily snapshots of the surface currents output from three data assimilative models in the trajectory models, in which tidal and inertial variations are not represented. To better examine the trajectory simulation on the shelf, we use the hourly surface currents output from the WFCOM realistic hindcast. Comparing Figures 6b and 6d, we can see that the WFCOM based trajectory model has higher skill scores than the GOM HYCOM based model in the inner and middle shelf areas. Similar improvement in the WFCOM based model is also seen in terms of the Lagrangian separation distances (Figure 8). Little improvement is seen in the zone near the open boundary, because the WFCOM is one-way nested within the GOM HYCOM, and the surface currents in that zone remain similar to those of the outer model. Despite the low

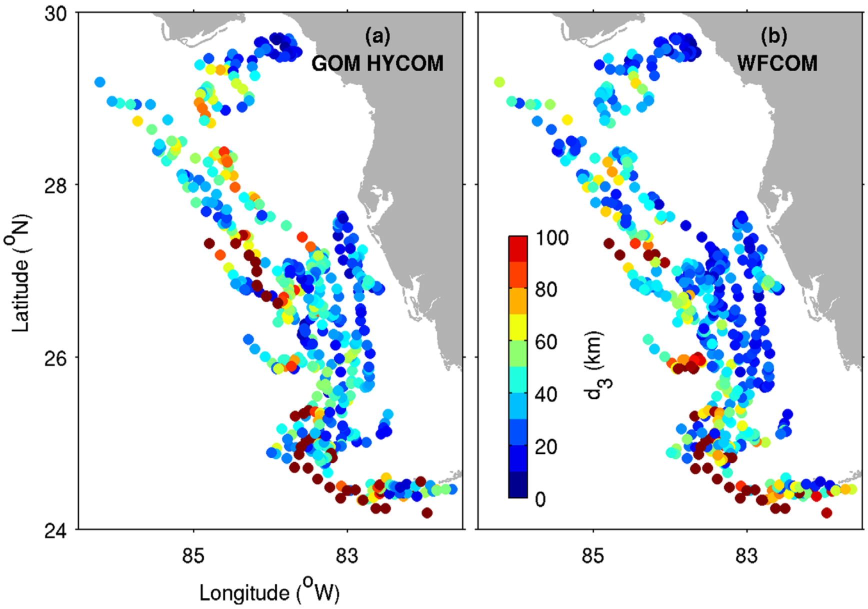

Figure 8. Spatial distribution of the Lagrangian separation distances (d_3) on the West Florida Shelf based on the surface currents output from (a) the Gulf of Mexico HYCOM and (b) the WFCOM. Note that smaller separation distances indicate better model performances.

skill scores near the open boundary, the WFCOM based trajectory model has an overall improvement than the GOM HYCOM based model, with the mean separation distance d_3 reduced from 41 to 38 km, and the mean skill score s_3 increased from 0.33 to 0.39 (Table 1). This improvement would be more significant if we only focus on the inner and middle shelf.

5. Summary

A series of altimetry-derived surface current products (OSCAR, GEKCO, and AVISO + different mean fields) are used to hindcast the drifter trajectories in the eastern Gulf of Mexico during May to August 2010. The performances of the trajectory models are gauged against the observed drifter trajectories in terms of Lagrangian separation distances (d_3) and a nondimensional skill score (s_3), respectively.

These altimetry-based trajectory models have about the same skills. After 3 days' simulation, the altimetry-based trajectory models have mean d values of 75–83 and 34–42 km (s values of 0.49–0.51 and 0.35–0.43) in the Gulf of Mexico deep water area and on the West Florida Continental Shelf, respectively. Adding surface wind Ekman components improves the AVISO-based model skills, especially over the shelf region.

Particularly within the transition zone from the deep ocean to the shelf, the altimetry-based trajectory models have higher skill scores than those based on the numerical models ($s_3 = 0.8$ versus $s_3 = 0.3$). This suggests that there may be benefit from additional data assimilation for the operational Global HYCOM, GOM HYCOM, and NCOM IASNFS in that transition zone.

Despite their limited temporal sampling, the altimetry-based trajectory models perform slightly better than those based on the data assimilative ocean circulation models in the deep ocean area of the GOM. This suggests that the altimetry products are useful for providing essential information on ocean surface currents for exploitation in water property transport, offshore oil and gas operations, hazardous spill mitigation, search and rescue, etc. With the development of a new generation of altimeters with higher resolution capabilities than their predecessors (e.g., CryoSat-2, AltiKa, Sentinel-3; SWOT) as well as the improvement of reprocessing in the coastal zone [see e.g., *Cipollini et al*., 2013 for a review], the altimetry products will find more practical applications of societal importance.

The altimetry-derived surface currents can describe only the present and past state of the surface currents, while ocean models can forecast the future state. This capability is needed in some applications, such as search and rescue and rapid response to oil spill emergencies [e.g., *Liu et al*., 2011c, 2011d]. Limited by data availability, only model hindcasts are used in this analysis. It would be useful to assess the predictive skills of the models using model forecast, which warrants future studies.

Acknowledgments
Present support is by NASA Ocean Surface Topography Science Team (OSTST) (award NNX13AE18G), NOAA through SECOORA, and BP/the Gulf of Mexico Research Initiative through the Deep-C Consortium. The success of drifter deployments from USF OCG is mainly attributed to J. Law, with assistance from FWC/FWRI, FIT, WHOI, and NEFSC (J. Manning). USF OCG staff J. Donovan, P. Smith, and D.A. Mayer assisted with drifter data processing, and L. Zheng assisted with WFCOM hindcast and analysis. Additional drifter data were provided by USCG. The AVISO products were produced by SSALTO/DUACS and distributed by AVISO, with support from CNES. The OSCAR data were obtained from JPL Physical Oceanography DAAC and developed by ESR. The GEKCO product used in this study was developed by Joël Sudre at LEGOS, France. The HYCOM model products were provided by the HYCOM Consortium and the IASNFS output was provided by the U.S. NRL via the web server of the Northern Gulf Institute. The wind product was provided by NCEP-NAM. This is CPR contribution 34.

References

Abascal, A. J., S. Castanedo, F. J. Mendez, R. Medina, and I. J. Losada (2009), Calibration of a Lagrangian transport model using drifting buoys deployed during the Prestige oil spill, *J. Coastal Res.*, *25*, 80–90.

Alvera-Azcárate, A., A. Barth, and R. H. Weisberg (2009), The surface circulation of the Caribbean Sea and the Gulf of Mexico as inferred from satellite altimetry, *J. Phys. Oceanogr.*, *39*, 640–657.

Barron, C. N., A. B. Kara, P. J. Martin, R. C. Rhodes, and L. F. Smedstad (2006), Formulation, implementation and examination of vertical coordinate choices in the global Navy Coastal Ocean Model (NCOM), *Ocean Modell.*, *11*, 347–375.

Barron, C. N., L. F. Smedstad, J. M. Dastugue, and O. M. Smedstad (2007), Evaluation of ocean models using observed and simulated drifter trajectories: Impact of sea surface height on synthetic profiles for data assimilation, *J. Geophys. Res.*, *112*, C07019, doi:10.1029/2006JC003982.

Barth, A., A. Alvera Azcarate, and R. H. Weisberg (2008), A nested model study of the loop current generated variability and its impact on the West Florida Shelf, *J. Geophys. Res.*, *113*, C05009, doi:10.1029/2007JC004492.

Bennett, N. D., et al. (2013), Characterising performance of environmental models, *Environ. Modell. Software*, *40*, 1–20.

Benveniste, J. (2011), Radar altimetry: Past, present and future, in *Coastal Altimetry*, edited by S. Vignudelli et al., pp. 1–17, Springer, Berlin, doi:10.1007/978-3-642-12796-0_1.

Birol, F., and C. Delebecque (2014), Using high sampling rate (10/20 Hz) altimeter data for the observation of coastal surface currents: A case study over the northwestern Mediterranean Sea, *J. Mar. Syst.*, *129*, 318–333, doi:10.1016/j.jmarsys.2013.07.009.

Bleck, R., D. H. C. Rooth, and L. Smith (1992), Salinity-driven thermocline transients in a wind- and thermohaline-forced isopycnic coordinate model of the North Atlantic, *J. Phys. Oceanogr.*, *22*, 1486–1505.

Bonjean, F., and G. S. E. Lagerloef (2002), Diagnostic model and analysis of the surface currents in the Tropical Pacific Ocean, *J. Phys. Oceanogr.*, *32*, 2938–2954.

Bouffard, J., F. Nencioli, R. Escudier, A. M. Doglioli, A. A. Petrenko, A. Pascual, P.-M. Poulain, and D. Elhmaidi (2014), Lagrangian analysis of satellite-derived currents: Application to the North Western Mediterranean coastal dynamics, *Adv. Space Res.*, *53*, 788–801.

Chang, Y.-L., and L.-Y. Oey (2013), Loop Current growth and eddy shedding using models and observations: Numerical process experiments and satellite altimetry data, *J. Phys. Oceanogr.*, *43*, 669–689.

Chassignet, E. P., and Z. D. Garraffo (2001), Viscosity parameterization and the gulf stream separation, in *Proceedings of 'Aha Huliko'a Hawaiian Winter Workshop on From Stirring to Mixing in a Stratified Ocean*, pp. 39–43, Univ. of Hawaii at Manoa, Honolulu.

Chassignet, E. P., H. E. Hurlburt, O. M. Smedstad, G. R. Halliwell, P. J. Hogan, A. J. Wallcraft, R. Baraille, and R. Bleck (2007), The HYCOM (HYbrid Coordinate Ocean Model) data assimilative system, *J. Mar. Syst.*, *65*, 60–83.

Chen, C., H. Liu, and R. C. Beardsley (2003), An unstructured, finite volume, three-dimensional, primitive equation ocean model: Application to coastal ocean and estuaries, *J. Atmos. Oceanic Technol.*, *20*, 159–186.

Cipollini, P., S. Vignudelli, F. Lyard, and L. Roblou (2008), 15 years of altimetry at various scales over the Mediterranean, in *Remote Sensing of the European Seas*, edited by V. Barale and M. Gade, pp. 295–306, Springer, Berlin.

Cipollini, P., et al. (2010), The role of altimetry in coastal observing systems, in *Proceedings of OceanObs'09: Sustained Ocean Observations and Information for Society, ESA Publ. WPP-306*, vol. 2, edited by J. Hall et al., ESRIN, Frascati, Italy, doi:10.5270/OceanObs09.cwp.16.

Cipollini, P., et al. (2013), Conquering the coastal zone: A new frontier for satellite altimetry, in *Proceedings of 20 Years of Progress in Radar Altimetry Symposium, Eur. Space Agency SP-710*, Noordwijk, Netherlands.

Cummings, J. A. (2005), Operational multivariate ocean data assimilation, *Q. J. R. Meteorol. Soc.*, *131*(613), 3583–3604.

Davis, R. E. (1985), Drifter observations of coastal surface currents during CODE: The method and descriptive view, *J. Geophys. Res.*, *90*, 4741–4755, doi:10.1029/JC090iC03p04741.

De Dominicis, M., N. Pinardi, G. Zodiatis, and R. Archetti (2013), MEDSLIK-II, a Lagrangian marine surface oil spill model for short-term forecasting—Part 2: Numerical simulations and validations, *Geosci. Model Dev.*, *6*, 1871–1888, doi:10.5194/gmd-6-1871-2013.

DiMarco, S. F., W. D. Nowlin Jr., and R. O. Reid (2005), A statistical description of the velocity Fields from upper ocean drifters in the Gulf of Mexico, in *Circulation in the Gulf of Mexico: Observations and Models, Geophys. Monogr. Ser.*, vol. 161, edited by W. Sturges and A. Lugo-Fernandez, pp. 101–110, AGU, Washington, D. C.

Dohan, K., and N. Maximenko (2010), Monitoring ocean currents with satellite sensors, *Oceanography*, *23*(4), 94–103.

Dohan, K., G. Lagerloef, F. Bonjean, L. Centurioni, M. Cronin, D. Lee, R. Lumpkin, N. Maximenko, and H. Uchida (2010), Measuring the global ocean surface circulation with satellite and in situ observations, in *Proceedings of the "OceanObs'09: Sustained Ocean Observations and Information for Society" Conference, ESA Publ. WPP-306*, vol. 2, edited by J. Hall et al., Eur. Space Agency, Venice, Italy.

Ducet, N., P. Y. Le Traon, and G. Reverdin (2000), Global high resolution mapping of ocean circulation from TOPEX/Poseidon and ERS-1 and −2, *J. Geophys. Res.*, *105*, 19,477–19,498.

Edwards, K. P., F. E. Werner, and B. O. Blanton (2006), Comparison of observed and modeled drifter trajectories in coastal regions: An improvement through adjustments for observed drifter slip and errors in wind fields, *J. Atmos. Oceanic Technol.*, *23*, 1614–1620, doi:10.1175/JTECH1933.1.

Fan, S., L.-Y. Oey, and P. Hamilton (2004), Assimilation of drifter and satellite data in a model of the Northeastern Gulf of Mexico, *Cont. Shelf Res.*, *24*, 1001–1013.

Fox, D. N., W. J. Teague, C. N. Barron, M. R. Carnes, and C. M. Lee (2002), The Modular Ocean Data Assimilation System (MODAS), *J. Atmos. Oceanic Technol.*, *19*, 240–252.

Fratantoni, D. M. (2001), North Atlantic surface circulation during the 1990's observed with satellite-tracked drifters, *J. Geophys. Res.*, *106*, 22,067–22,093.

Fu, L.-L., and D. B. Chelton (1984), Temporal variability of the Antarctic Circumpolar Current observed from satellite altimetry, *Science*, *226*, 343–346.

Garraffo, Z. D., A. J. Mariano, A. Griffa, C. Veneziani, and E. P. Chassignet (2001), Lagrangian data in a high-resolution numerical simulation of the North Atlantic, I. Comparison with in situ drifter data, *J. Mar. Syst.*, *29*(1–4), 157–176.

Griffa, A., A. D. Kirwan, A. J. Mariano, T. M. Özgökmen, and T. Rossby (2007), *Lagrangian Analysis and Prediction of Coastal and Ocean Dynamics*, 487 pp., Cambridge Univ. Press, U. K.

Halliwell, G., A. Srinivasan, V. Kourafalou, H. Yang, D. Willey, M. Le Hénaff, and R. Atlas (2014), Rigorous evaluation of a fraternal twin ocean OSSE system for the Open Gulf of Mexico, *J. Atmos. Oceanic Technol.*, *31*, 105–130, doi:10.1175/JTECH-D-13-00011.1.

Hamilton, P., K. A. Donohue, R. R. Leben, A. Lugo-Fernández, R. E. Green (2011), Loop Current observations during spring and summer of 2010: Description and historical perspective, in *Monitoring and Modeling the Deepwater Horizon Oil Spill: A Record-Breaking Enterprise, Geophys. Monogr. Ser., vol*. 195, edited by Y. Liu et al., pp. 117–130, AGU, Washington D. C., doi:10.1029/2011GM001116.

Hamilton, P., G. S. Fargion, and D. C. Biggs (1999), Loop current eddy paths in the western Gulf of Mexico, *J. Phys. Oceanogr.*, *29*, 1180–1207.

Han, G. (2007), Satellite observations of seasonal and interannual changes of sea level and currents over the Scotian Slope, *J. Phys. Oceanogr.*, *37*, 1051–1065.

He, R., Y. Liu, and R. H. Weisberg (2004), Coastal Ocean wind fields gauged against the performance of an ocean circulation model, *Geophys. Res. Lett.*, *31*, L14303, doi:10.1029/2003GL019261.

Helber, R. W., R. H. Weisberg, F. Bonjean, E. S. Johnson, and G. S. E. Lagerloef (2007), Satellite-derived surface current divergence in relation to Tropical Atlantic SST and wind, *J. Phys. Oceanogr.*, *37*, 1357–1375.

Hofmann, E. E., K. S. Hedstrom, J. R. Moisan, D. B. Haidvogel, and D. L. Mackas (1991), Use of simulated drifter tracks to investigate general transport patterns and residence times in the coastal transition zone, *J. Geophys. Res.*, *96*, 15,041–15,052.

Ivichev, I., L. R. Hole, L. Karlin, C. Wettre, and J. Röhrs (2012), Comparison of operational oil spill trajectory forecasts with surface drifter trajectories in the Barents Sea, *J. Geol. Geosci.*, *1*, 105, doi:10.4172/jgg.1000105.

Jacobs, G. A., and R. R. Leben (1990), Loop current eddy shedding estimated using Geosat altimeter data, *Geophys. Res. Lett.*, *17*, 2385–2388.

Janeiro, J., A. Zacharioudaki, E. Sarhadi, A. Neves, F. Martins (2014), Enhancing the management response to oil spills in the Tuscany Archipelago through operational modelling, *Mar. Pollut. Bull.*, doi:10.1016/j.marpolbul.2014.03.021, in press.

Johnson, E. S., F. Bonjean, G. S. E. Lagerloef, J. T. Gunn, and G. T. Mitchum (2007), Validation and error analysis of OSCAR sea surface currents, *J. Atmos. Oceanic Technol.*, *24*, 688–701. doi:10.1175/JTECH1971.1.

Kirwan, A. D., Jr., J. K. Lewis, A. W. Indest, P. Reinersman, and I. Quintero (1988), Observed and simulated kinematic properties of loop current rings, *J. Geophys. Res.*, *93*, 1189–1198.

Ko, D. S., R. H. Preller, and P. J. Martin (2003), An experimental real-time Intra Americas Sea Ocean Nowcast/Forecast System for coastal prediction, in *Proceedings of AMS 5th Conference on Coastal Atmospheric & Oceanic Prediction & Processes*, pp. 97–100, AMS, Washington, D. C.

Ko, D. S., P. J. Martin, C. D. Rowley, and R. H. Preller (2008), A real-time coastal ocean prediction experiment for MREA04, *J. Mar. Syst.*, *69*, 17–28, doi:10.1016/j.jmarsys.2007.02.022.

Kuznetsov, L., M. Toner, A. D. Kirwan, C. K. R. T. Jones, L. Kantha, and J. Choi (2002), The Loop Current and adjacent rings delineated by Lagrangian analysis of the near surface flow, *J. Mar. Res.*, *60*, 405–429.

LaCasce, J. H., and C. Ohlmann (2003), Relative dispersion at the surface of the Gulf of Mexico, *J. Mar. Res.*, *61*, 285–312.

Lagerloef, G. S. E., G. T. Mitchum, R. Lukas, and P. Niiler (1999), Tropical Pacific near surface currents estimated from altimeter, wind and drifter data, *J. Geophys. Res.*, *104*, 23,313–23,326.

Lagerloef, G. S. E., R. Lukas, F. Bonjean, J. T. Gunn, G. T. Mitchum, M. Bourassa, and A. J. Busalacchi (2003), El Niño Tropical Pacific Ocean surface current and temperature evolution in 2002 and outlook for early 2003, *Geophys. Res. Lett.*, *30*(10), 1514, doi:10.1029/2003GL017096.

Leben, R. R., and G. H. Born (1993), Tracking Loop Current eddies with satellite altimetry, *Adv. Space Res.*, *13*, 325–333.

Legeckis, R., C. W. Brown, F. Bonjean, and E. S. Johnson (2004), The influence of tropical instability waves on phytoplankton blooms in the wake of the Marquesas Islands during 1998 and on the currents observed during the drift of the Kon-Tiki in 1947, *Geophys. Res. Lett.*, *31*, L23307, doi:10.1029/2004GL021637.

Le Traon, P. Y., and F. Hernandez (1992), Mapping the oceanic mesoscale circulation: Validation of satellite altimetry using surface drifters, *J. Atmos. Oceanic Technol.*, *9*, 687–698.

Le Traon, P.-Y., and R. A. Morrow (2001), Ocean currents and mesoscale eddies. Satellite Altimetry and Earth sciences, in *A Handbook of Techniques and Applications*, edited by L.-L. Fu and A. Cazenave, pp. 171–215, Academic, London, UK.

Le Traon, P. Y., Y. Faugere, F. Hernandez, J. Dorandeu, F. Merttz, and M. Ablain (2003), Can we merge GEOSAT-follow-on with TOPEX/Poseidon and ERS-2 for an improved description of the ocean circulation? *J. Atmos. Oceanic Technol.*, *20*, 889–895.

Liu, Y., and R. H. Weisberg (2005), Patterns of ocean current variability on the West Florida Shelf using the self-organizing map, *J. Geophys. Res.*, *110*, C06003, doi:10.1029/2004JC002786.

Liu, Y., and R. H. Weisberg (2007), Ocean currents and sea surface heights estimated across the West Florida Shelf, *J. Phys. Oceanogr.*, *37*, 1697–1713, doi:10.1175/JPO3083.1.

Liu, Y., and R. H. Weisberg (2011), Evaluation of trajectory modeling in different dynamic regions using normalized cumulative Lagrangian separation, *J. Geophys. Res.*, *116*, C09013, doi:10.1029/2010JC006837.

Liu, Y., R. H. Weisberg, and Y. Yuan (2008), Patterns of upper layer circulation variability in the South China Sea from satellite altimetry using the self-organizing map, *Acta Oceanol. Sin.*, *27*(suppl.), 129–144.

Liu, Y., A. MacFadyen, Z.-G. Ji, and R. H. Weisberg (Eds.) (2011a), Monitoring and modeling the Deepwater Horizon oil spill: A record-breaking enterprise, *Geophys. Monogr. Ser.*, vol. 195, p. 271, AGU, Washington, D. C., doi:10.1029/GM195.

Liu, Y., R. H. Weisberg, C. Hu, C. Kovach, and R. Riethmüller (2011b), Evolution of the Loop Current system during the Deepwater Horizon oil spill event as observed with drifters and satellites, in *Monitoring and Modeling the Deepwater Horizon Oil Spill: A Record-Breaking Enterprise*, *Geophys. Monogr. Ser.*, vol. 195, edited by Y. Liu et al., pp. 91–101, AGU, Washington, D.C., doi:10.1029/2011GM001127.

Liu, Y., R. H. Weisberg, C. Hu, and L. Zheng (2011c), Tracking the Deepwater Horizon oil spill: A modeling perspective, *Eos Trans. AGU*, *92*(6), 45–46, doi:10.1029/2011EO060001.

Liu, Y., R. H. Weisberg, C. Hu, and L. Zheng (2011d), Trajectory forecast as a rapid response to the *Deepwater Horizon* oil spill, in *Monitoring and Modeling the Deepwater Horizon Oil Spill: A Record-Breaking Enterprise*, *Geophys. Monogr. Ser.*, vol. *195*, edited by Y. Liu et al., pp. 153–165, AGU, Washington, D. C., doi:10.1029/2011GM001121.

Liu, Y., R. H. Weisberg, S. Vignudelli, L. Roblou, and C. Merz (2012), Comparison of the X-TRACK altimetry estimated currents with moored ADCP and HF radar observations on the West Florida Shelf, *Adv. Space Res.*, *50*(8), 1085–1098, doi:10.1016/j.asr.2011.09.012.

Lugo-Fernandez, A., K. J. P. Deslarzes, J. M. Price, G. S. Boland, and M. V. M. V. Morin (2001), Inferring probable dispersal of Flower Garden Banks coral larvae (Gulf of Mexico) using observed and simulated drifter trajectories, *Cont. Shelf Res.*, *21*, 47–67.

Lumpkin, R., G. Goni, and K. Dohan (2010), Surface currents, in "State of the Climate in 2009," *Bull. Am. Meteorol. Soc.*, *91*, S65–S69.

McClean, J. L., P.-M. Poulain, and J. W. Pelton (2002), Eulerian and Lagrangian statistics from surface drifters and a high-resolution simulation in the North Atlantic, *J. Phys. Oceanogr.*, *32*, 2472–2491.

Miller, L., and J. Kuhn (2010), Evaluation of altimeter observations and model forecasts of the Gulf of Mexico oil spill, paper presented at the 4th Coastal Altimetry Workshop, European Space Agency/The US National Aeronautics and Space Administration/The US National Oceanic and Atmospheric Administration, Porto, Portugal.

Mitchum, G. T., and W. Sturges (1982), Wind-driven currents on the West Florida Shelf, *J. Phys. Oceanogr.*, *12*, 1310–1317.

Mooers, C. N. K., E. D. Zaron, and M. K. Howard (2012), *Final Report for Phase I of Gulf of Mexico 3-D Operational Ocean Forecast System Pilot Prediction Project (GOMEX-PPP)*, U. S. Dep. of Energy, Washington, D. C.

Morey, S. L., J. Zavala-Hidalgo, and J. J. O'Brien (2005), The seasonal variability of continental shelf circulation in the northern and western Gulf of Mexico from a high resolution numerical model, in *Circulation in the Gulf of Mexico: Observations and Models, Geophys. Monogr. Ser.*, vol. 161, pp. 203–218.

Oey, L.-Y., T. Ezer, and H.-C. Lee (2005), Loop Current, rings and related circulation in the Gulf of Mexico: A review of numerical models and future challenges, in *Circulation in the Gulf of Mexico: Observations and Models, Geophys. Monogr. Ser.*, vol. 161, edited by W. Sturges and A. Lugo-Fernández, pp. 31–56, AGU, Washington, D. C.

Ohlmann, J. C., and S. Mitarai (2010), Lagrangian assessment of simulated surface current dispersion in the coastal ocean, *Geophys. Res. Lett.*, *37*, L17602, doi:10.1029/2010GL044436.

Olascoaga, M. J., et al. (2013), Drifter motion in the Gulf of Mexico constrained by altimetric Lagrangian Coherent Structures, *Geophys. Res. Lett.*, *40*, 6171–6175, doi:10.1002/2013GL058624.

Özgökman, T. M., A. Griffa, A. J. Mariano, and L. I. Piterbarg (2000), On the predictability of Lagrangian trajectories in the ocean, *J. Atmos. Oceanic Technol.*, *17*, 366–383.

Pascual, A., Y. Gaugere, G. Larnicol, and P. Y. LeTraon (2006), Improved description of the ocean mesoscale variability by combining four satellite altimeters, *Geophys. Res. Lett.*, *33*, L02611, doi:10.1029/2005GL024633.

Picaut, J., E. Hackert, A. J. Busalacchi, R. Murtugudde, and G. S. E. Lagerloef (2002), Mechanisms of the 1997–1998 El Nino-La Nina, as inferred from space-based observations, *J. Geophys. Res.*, *107*(C5), 3037, doi:10.1029/2001JC000850.

Price, J. M., et al. (2006), Preliminary assessment of an oil-spill trajectory model using satellite-tracked, oil-spill-simulating drifters, *Environ. Modell. Software*, *21*, 258–270.

Rio, M. H., and F. Hernandez (2004), A mean dynamic topography computed over the world ocean from altimetry, in-situ measurements and a geoid model, *J. Geophys. Res.*, *109*, C12032, doi:10.1029/2003JC002226.

Rio, M. H., P.-M. Poulain, A. Pascal, E. Mauri, G. Larnicol, and R. Santoleri (2007), A mean dynamic topography of the Mediterranean Sea computer from altimeter data, in situ measurements and a general circulation model, *J. Mar. Syst.*, *65*, 484–508.

Rio, M. H., P. Schaeffer, G. Moreaux, J.-M. Lemoine, and E. Bronner (2009), A new mean dynamic topography computed over the global ocean from GRACE data, altimetry and in-situ measurements, poster communication presented at OceanObs09 symposium, IOC/UNESCO, Venice, 21–25 Sep.

Rio, M. H., S. Guinehut, and G. Larnicol (2011), New CNES-CLS09 global mean dynamic topography computed from the combination of GRACE data, altimetry, and in situ measurements, *J. Geophys. Res.*, *116*, C07018, doi:10.1029/2010JC006505.

Robinson, M. J. (2011), Improvements to a real-time, satellite-derived surface current product (OSCAR) and evaluation in the intra-American Sea, MSc Thesis, Univ. of South Florida, St. Petersburg, Fla.

Rogers, E., et al. (2009), The NCEP North American Mesoscale Modeling System: Recent changes and future plans, paper presented at the 23rd Conference on Weather Analysis and Forecasting/19th Conference on Numerical Weather Prediction, Am. Meteorol. Soc., Washington, D. C.

Röhrs, J., K. H. Christensen, L. R. Hole, G. Broström, M. Drivdal, and S. Sundby (2012), Observation-based evaluation of surface wave effects on currents and trajectory forecasts, *Ocean Dyn.*, *62*, 1519–1533.

Rosmond, T. E., J. Teixeira, M. Peng, T. F. Hogan, and R. Pauley (2002), Navy operational global atmospheric prediction system (NOGAPS): Forcing for ocean models, *Oceanography*, *15*, 99–108.

Sayol, J. M., A. Orfila, G. Simarro, D. Conti, L. Renault, and A. Molcard (2014), A Lagrangian model for tracking surface spills and SaR operations in the ocean, *Environ. Modell. Software*, *52*, 74–82, doi:10.1016/j.envsoft.2013.10.013.

Sotillo, M. G., et al. (2008), Towards an operational system for oil-spill forecast over Spanish waters: Initial developments and implementation test, *Mar. Pollut. Bull.*, *56*, 686–703.

Stewart, R. H. (2008), *Introduction to Physical Oceanography*, Tex. A&M Univ., College Station. [Available at http://oceanworld.tamu.edu/resources/ocng_textbook/PDF_files/book.pdf.]

Sturges, W., and A. Lugo-Fernandez (Eds.) (2005), Circulation in the Gulf of Mexico: Observations and models, *Geophys. Monogr. Ser.*, vol. 161, pp. 360, AGU, Washington, D. C.

Sudre, J., and R. Morrow (2008), Global surface currents: A high resolution product for investigating ocean dynamics, *Ocean Dyn.*, *58*, 101–118, doi:10.1007/s10236-008-0134-9.

Sudre, J., C. Maes, and V. Garcon (2013), On the global estimates of geostrophic and Ekman surface currents, *Limnol. Oceanogr. Methods*, *3*, 1–20, doi:10.1215/21573689-2071927.

Toner, M., A. D. Kirwan Jr., L. H. Kantha, and J. K. Choi (2001), Can general circulation models be assessed and their output enhanced with drifter data?, *J. Geophys. Res.*, *106*, 19,563–19,579, doi:10.1029/2000JC000587.

Vignudelli, S., A. G. Kostianoy, P. Cipollini, and J. Benveniste (Eds.) (2011), *Coastal Altimetry*, 1st ed., 566 pp., Springer, New York.

Walker, N. D., et al. (2011), Loop Current cyclonic eddy merger impacts 2010 Gulf of Mexico oil spill, in *Monitoring and Modeling the Deepwater Horizon Oil Spill: A Record-Breaking Enterprise*, *Geophys. Monogr. Ser.*, vol. 195, edited by Y. Liu et al., pp. 103–116, AGU, Washington, D. C., doi:10.1029/2011GM001120.

Wei, M., G. Jacobs, C. Rowley, C. N. Barron, P. Hogan, P. Spence, O. M. Smedstad, P. Matine, P. Muscarella, and E. Coelho (2014), The performance of the US Navy's RELO ensemble, NCOM, HYCOM during the period of GLAD at-sea experiment in the Gulf of Mexico, *Deep Sea Res., Part II*, doi:10.1016/j.dsr2.2013.09.002, in press.

Weisberg, R. H. (2011), Coastal ocean pollution, water quality and ecology: A commentary, *MTS J.*, *45*(2), 35–42.

Weisberg, R. H., Z. Li, and F. E. Muller-Karger (2001), West Florida shelf response to local wind forcing: April 1998, *J. Geophys. Res.*, *106*, 31,239–31,262.

Weisberg, R. H., R. He, Y. Liu, and J. Virmani (2005), West Florida shelf circulation on synoptic, seasonal, and inter-annual time scales, in *Circulation in the Gulf of Mexico: Observations and Models, Geophys. Monogr. Ser.* 161, 325–347, AGU, Washington, D. C.

Weisberg, R. H., Y. Liu, and D. A. Mayer (2009), West Florida Shelf mean circulation observed with long-term moorings, *Geophys. Res. Lett.*, *36*, L19610, doi:10.1029/2009GL040028.

Weisberg, R. H., L. Zheng, Y. Liu, S. Murawski, C. Hu, and J. Paul (2014), Did Deepwater Horizon hydrocarbons transit to the west Florida continental shelf? *Deep Sea Res., Part II*, doi:10.1016/j.dsr2.2014.02.002, in press.

Winant, C. D., D. J. Alden, E. P. Dever, K. A. Edwards, and M. C. Hendershott (1999), Near-surface trajectories off central and southern California, *J. Geophys. Res.*, *104*, 15,713–15,726, doi:10.1029/1999JC900083.
Willis, J. K., and L.-L. Fu (2008), Combining altimeter and subsurface float data to estimate the time-averaged circulation in the upper ocean, *J. Geophys. Res.*, *113*, C12017, doi:10.1029/2007JC004690.
Yang, H., R. H. Weisberg, P. P. Niiler, W. Sturges, and W. Johnson (1999), Lagrangian circulation and forbidden zone on the west Florida shelf, *Cont. Shelf Res.*, *19*, 1221–1245.
Yaremchuk, M., P. Spence, M. Wei, and G. Jacobs (2014), Lagrangian predictability in the DWH region from HF radar observations and model output, *Deep Sea Res., Part II*, doi:10.1016/j.dsr2.2013.05.035.
Zheng, L., and R. H. Weisberg (2012), Modeling the west Florida coastal ocean by downscaling from the deep ocean, across the continental shelf and into the estuaries, *Ocean Modell.*, *48*, 10–29, doi:10.1016/j.ocemod.2012.02.002.